

Efficient Learning of Affine and Rational Dependency LPV Models With Linear Fractional Representation ^{*}

Roel Drenth^{*} Jan H. Hoekstra^{*} Maarten Schoukens^{*}
Roland Tóth^{*,**}

^{*} Control Systems Group, Dept. of Electrical Eng., Eindhoven University of Technology, Eindhoven, The Netherlands. (e-mail: {r.drenth, j.h.hoekstra, m.schoukens, r.toth}@tue.nl).

^{**} Systems and Control Laboratory, HUN-REN Institute for Computer Science and Control, Budapest, Hungary

Abstract: Identifying control-friendly models of nonlinear systems remains one of the major challenges at the intersection of system identification and control. The *Linear Parameter-Varying* (LPV) framework offers a promising solution, but existing identification methods often rely on model structures with affine scheduling dependency. Instead, this work proposes the use of LPV models with *Linear Fractional Representation* (LFR) admitting a rational scheduling-dependency, capable of modelling complex nonlinear systems with fewer scheduling variables compared to affine models. This work introduces a direct parameterization to ensure well-posedness of rational LPV-LFR models, which by joint-estimation of an LPV plant and scheduling map, using only input-output data, is capable of modelling complex nonlinear systems. Accuracy of the proposed approach is shown on two simulation examples.

Keywords: Linear Parameter-Varying System Identification, Linear Fractional Representation, Scheduling Map Estimation

1. INTRODUCTION

As the performance demands of systems in engineering grow, the limitations of the ubiquitous *Linear Time-Invariant* (LTI) assumptions become apparent. Employing the LTI framework to model systems which are often inherently *nonlinear* (NL) results in models with limited accuracy, which subsequently limits achievable performance in (model-based) control.

The *Linear Parameter-Varying* (LPV) framework offers an attractive alternative to the LTI framework. LPV models retain a structure that is linear in the input, but the model parameters can vary as a function of a *scheduling variable*. Through change in the scheduling variable, LPV models are capable of representing time-varying and nonlinear behaviour. This results in a model class which provides a middle-ground between the limitations of the LTI class and the complexity of nonlinear models. Importantly, the LPV structure enables controller synthesis tools with performance guarantees (see e.g., Mohammadpour and Scherer (2012)). Moreover, the LPV framework enjoys the support of various software toolboxes, implementing

powerful control and modelling approaches (Hjartarson et al., 2015; den Boef et al., 2021).

Traditional LPV identification methods, which require knowledge of the scheduling signal, are often extensions of their LTI counterparts. Notable methods include *Prediction Error Minimization* (PEM) methods (see e.g., Tóth (2010)), and *Subspace Identification* (see e.g., Van Wingerden and Verhaegen (2009), Cox and Tóth (2021)). In recent years, methods which jointly identify an LPV model and its scheduling map have been gaining attention. By estimating the scheduling map directly from data, the often significant challenge of modelling the scheduling is bypassed. In particular, *deep-learning*-based identification methods with LPV-*state-space* (SS) models and *Neural Network* (NN) scheduling maps have been shown to efficiently estimate LPV/NL models (Verhoek et al., 2022) and noise processes (Bemporad and Tóth, 2025).

LPV identification methods have been developed for a wide range of model classes, including LPV-*Input-Output* (IO), LPV-SS and LPV-*Linear Fractional Representation* (LFR) classes. However, the LPV-SS and LPV-LFR model classes are most commonly used for controller synthesis. For LPV-SS models, controller synthesis methods require affine dependency on the scheduling variables. Using a simple affine-dependency structure to model complex nonlinearities often comes with the trade-off of requiring increased number of scheduling variables and a complex scheduling map, which in turn can introduce unnecessary conservatism in controller synthesis, called overbounding.

^{*} This work is funded by the European Union (ERC, COMPLETE, 101075836), by the Air Force Office of Scientific Research under award number FA8655-23-1-7061, and the Mathworks Inc. Views and opinions expressed are however those of the author(s) only and do not necessarily reflect those of the European Union or the European Research Council Executive Agency. Neither the European Union nor the granting authority can be held responsible for them.

Alternatively, we consider the LPV-LFR class of models. This class admits rational dependency on the scheduling variable which can reduce the required dimension and complexity of the scheduling map and thus the effects of overbounding (see e.g., Hoffmann and Werner (2014) for a comparison). Importantly, this model class is still suited for controller synthesis (Scherer (2001)). However, identification of LPV-LFR models corresponding to rational-dependency is a significantly more challenging problem as the rational terms can introduce singularities.

So far, little research on the identification of LPV-LFR models has been performed, and the methods that do exist face significant challenges, such as requiring full-state measurements (Nemani et al. (1995)), being restricted to affine-dependency (Mejari et al. (2019); Bianchi and Sánchez-Peña (2010)), or assuming models cannot be ill-posed (Lee and Poolla (1999), Cheng and Sznajder (2015)). In particular, to the best of the authors' knowledge, no methods to ensure well-posedness in identification of LPV-LFR models under rational scheduling dependency exist. Furthermore, no research on the use of LPV-LFR models in the aforementioned joint scheduling and model identification setting has been performed.

In this work we leverage the efficiency of *deep-learning*-based joint-estimation methods with the expressivity of rational LPV-LFR models to estimate nonlinear models. Specifically, as main contribution, we provide a direct parameterization of LPV-LFR models that guarantees well-posedness, inspired by direct parameterizations for stability of recurrent models (Revay et al. (2020), Verhoek et al. (2023)).

The remainder of this paper first discusses the problem setting, including the model structure, in Section 2. Next, in Section 3, well-posedness conditions and a direct-parameterization satisfying such conditions is introduced. This is followed by the introduction of the identification methodology in Section 4. Finally, the proposed method is evaluated on simulation examples in Section 5, after which conclusions are drawn in Section 6.

2. PROBLEM SETTING

2.1 Data-generating system

We consider *discrete-time* (DT) data-generating systems with the following state-space representation:

$$\Sigma_o : \begin{cases} x_{k+1} = f(x_k, u_k), \\ y_k = g(x_k, u_k) + e_k, \end{cases} \quad (1)$$

where $k \in \mathbb{Z}$ is the discrete time, where $x_k \in \mathbb{X} \subseteq \mathbb{R}^{n_x}$ is the state of the plant, $u_k \in \mathbb{U} \subseteq \mathbb{R}^{n_u}$ is the input signal, $y_k \in \mathbb{Y} \subseteq \mathbb{R}^{n_y}$ is the system output, with output-additive white noise $e_k \in \mathbb{E} \subseteq \mathbb{R}^{n_y}$. u_k is assumed to be quasi-stationary. The state transition function $f : \mathbb{X} \times \mathbb{U} \rightarrow \mathbb{X}$ and output function $g : \mathbb{X} \times \mathbb{U} \rightarrow \mathbb{Y}$ are considered to be deterministic and nonlinear.

2.2 Linear Fractional Representation

The *Linear Fractional Representation* is a general model representation that allows one to model dynamical systems

with a wide range of properties, such as nonlinearities and uncertainty, in a unified manner. It originally gained popularity in the field of robust control (Zhou et al. (1996)) where it is used to model uncertain systems. For LPV systems it is instead used to incorporate the parameter-varying nature. With an LFR, LPV systems are represented by interconnections between nominal systems M and their parameter-varying components represented by matrix functions $\Delta(p)$ with linear dependence on the scheduling signal p (Scherer and Weiland, 2015).

Let us define an LPV-LFR as a pair $\{M, \Delta(p)\}$ where the interconnection in discrete time follows the standard form:

$$M : \begin{cases} \begin{bmatrix} x_{k+1} \\ z_k \\ y_k \end{bmatrix} = \begin{bmatrix} A_x & B_w & B_u \\ C_z & D_{zw} & D_{zu} \\ C_y & D_{yw} & D_{yu} \end{bmatrix} \begin{bmatrix} x_k \\ w_k \\ u_k \end{bmatrix}, \\ w_k = \Delta(p_k)z_k, \end{cases} \quad (2)$$

where $w_k, z_k \in \mathbb{R}^{n_w}$ are the latent variables, A_x, \dots, D_{yu} are real matrices of appropriate dimensions, and $p_k \in \mathbb{P} \subseteq \mathbb{R}^{n_p}$ is the scheduling variable. The matrix function $\Delta(p_k) : \mathbb{P} \rightarrow \mathbb{R}^{n_w \times n_w}$, commonly referred to as the Delta-block, is typically assumed to be diagonal and can be defined as:

$$\Delta(p_k) = \begin{bmatrix} p_{1,k} I_{\eta_1} & & 0 \\ & \ddots & \\ 0 & & p_{n_p,k} I_{\eta_{n_p}} \end{bmatrix}, \quad (3)$$

where η is a vector of integers denoting the number of repetitions per scheduling variable and where $I_{\eta_1}, \dots, I_{\eta_{n_p}}$ are identity matrices of appropriate size to realize the correct total dimension of $\Delta(p_k)$. This interconnection is equivalent to a LPV-SS representation with rational dependency on p_k :

$$\begin{bmatrix} x_{k+1} \\ y_k \end{bmatrix} = \begin{bmatrix} \mathcal{A}(p_k) & \mathcal{B}(p_k) \\ \mathcal{C}(p_k) & \mathcal{D}(p_k) \end{bmatrix} \begin{bmatrix} x_k \\ u_k \end{bmatrix}, \quad (4)$$

where $\mathcal{A}(p_k), \mathcal{B}(p_k), \mathcal{C}(p_k), \mathcal{D}(p_k)$ are matrix functions of p_k .

This is achieved by eliminating the latent variables w_k and z_k in (2) by substitution of

$$z_k = (I - D_{zw}\Delta(p_k))^{-1}(C_z x_k + D_{zu} u_k). \quad (5)$$

Which requires $(I - D_{zw}\Delta(p_k))$ to be non-singular. This gives rise to the following definition:

Definition 1. The LPV-LFR model defined by the pair $\{M, \Delta(p_k)\}$ according to (2) is *well-posed*, if $I - D_{zw}\Delta(p_k)$ is non-singular, i.e., $\det(I - D_{zw}\Delta(p_k)) \neq 0$ for all possible realizations of the scheduling variable, i.e., $p_k \in \mathbb{P}$.

As this representation admits rational LPV-SS models, it is a generalization of commonly used affine LPV-SS models. Notably, affine-dependency models are represented by taking (2) with $D_{zw} = 0$, resulting in a model set which is always well-posed. Furthermore, given an LPV-SS model with affine dependency an equivalent LPV-LFR realization can easily be recovered using *Singular Value Decomposition* (SVD) methods (Zhou et al., 1996).

LPV-LFR models can be used to represent LPV systems by considering p_k to be an exogenous signal. Nonlinear systems such as Σ_o in (1) require defining $p_k = \psi(x_k, u_k)$ where $\psi : \mathbb{R}^{n_x} \times \mathbb{R}^{n_u} \rightarrow \mathbb{R}^{n_p}$ is a *scheduling map*, corresponding to a LPV embedding of the original nonlinear system.

2.3 Identification structure

We aim to identify the data-generating NL system Σ_0 based on a dataset \mathcal{D}_N , in the form of parameterized surrogate model. Specifically, we consider *self-scheduled* LPV-LFR models, requiring the joint-estimation of LPV model and scheduling map, similar to Verhoek et al. (2022), which treats the LPV-SS setting.

We parameterize the surrogate model for the system (1) in an LPV-LFR form according to:

$$G_\theta : \begin{cases} \begin{bmatrix} \hat{x}_{k+1} \\ \hat{z}_k \\ \hat{y}_k \end{bmatrix} = \begin{bmatrix} A_x & B_w & B_u \\ C_z & D_{zw} & D_{zu} \\ C_y & D_{yw} & D_{yu} \end{bmatrix} \begin{bmatrix} \hat{x}_k \\ \hat{w}_k \\ u_k \end{bmatrix}, \\ \hat{w}_k = \Delta(\hat{p}_k)\hat{z}_k, \end{cases} \quad (6)$$

where the matrices A_x, \dots, D_{yu} form the parameter vector θ_G . Next, we consider the scheduling signal \hat{p}_k to be defined by a scheduling map $\hat{\psi}_\theta(x_k, u_k, d_k)$, where $d_k \in \mathbb{R}^{n_d}$ is a known exogenous signal. The inclusion of d_k allows for full or partial external scheduling. To be able to capture the set of data-generating systems described in (1), the scheduling map is required to be a general function approximator. To achieve this, we propose the use of a *Feedforward Neural Network* (FNN) parameterization of the scheduling map. Typically the FNN is extended with a linear bypass layer, resulting in a one-block ResNet (He et al., 2016). This bypass aids in the learning of linear dependencies on x_k, u_k and d_k if present. The weights and biases of the ResNet form the parameter vector θ_ψ . For mildly nonlinear systems, the authors suggest the use of a ResNet with two hidden layers, limited amount of neurons per layer (6-12) and hyperbolic tangent (tanh) activation functions.

3. ENSURING WELL-POSEDNESS

3.1 Well-posedness conditions

As we have shown in (5), for an LPV-LFR to be well-posed, we require $I - D_{zw}\Delta(p_k)$ to be non-singular for all possible realizations of the scheduling variables, i.e., $p_k \in \mathbb{P}$. We propose a novel method for guaranteeing well-posedness of LPV-LFR models, we begin by establishing key assumptions and conditions that play a role in this result.

Assumption 2. The matrix function $\Delta(p_k)$ has a diagonal structure as defined in (3).

Assumption 3. The scheduling set¹ \mathbb{P} is contained in the closed n_p -dimensional ℓ_∞ unit ball, i.e.,

$$\mathbb{P} \subseteq \{p : \mathbb{Z} \rightarrow \mathbb{R}^{n_p} \mid \|p_k\|_\infty \leq 1 \forall k \in \mathbb{Z}\}. \quad (7)$$

It is important to note that Assumption 3 is not restrictive. Given an arbitrary, well-posed, LFR $\{G, \Delta(p)\}$, under Assumption 2 it is trivial to retrieve an equivalent LFR defined by the pair $\{\bar{M}, \bar{\Delta}(p)\}$ which satisfies Assumption 3 by scaling and shifting the scheduling variables (see e.g., Scherer and Weiland (2015)). For models with NN scheduling map this can be enforced through the incorporation of an activation function on the output layer, such as the tanh function.

¹ One could also assume constraints directly on the scheduling map, however by constraining the scheduling set the results also hold for externally scheduled LPV models.

Definition 4. The *spectral radius* ρ of a matrix $A \in \mathbb{R}^{n \times n}$ with eigenvalues $\lambda_1, \dots, \lambda_n$ is defined as:

$$\rho(A) = \max\{|\lambda_1|, \dots, |\lambda_n|\}. \quad (8)$$

Condition 5. The spectral radius ρ of D_{zw} is strictly smaller than 1, i.e.,

$$\rho(D_{zw}) < 1. \quad (9)$$

These lead to the following theorem.

Theorem 6. If Assumptions 2, 3, and Condition 5 hold, the LPV-LFR model (2) is well-posed.

Proof. From Assumptions 2 and 3 it follows that $\rho(\Delta(p_k)) \leq 1, \forall p_k \in \mathbb{P}$. Additionally, under Assumption 2, it holds that $\rho(D_{zw}\Delta(p_k)) \leq \rho(D_{zw})\rho(\Delta(p_k))$. Thus, it follows that $I - D_{zw}\Delta(p_k) \succ 0$ for all combinations of $p_k \in \mathbb{P}$. This implies $\det(I - D_{zw}\Delta(p_k)) > 0, \forall p_k \in \mathbb{P}$, satisfying the well-posedness condition.

3.2 Well-posedness by direct parameterization

To ensure Condition 5 is satisfied, we define

$$D_{zw} = e^{-N}, \quad N \succ 0. \quad (10)$$

As the matrix exponential maps eigenvalues λ to e^λ , the originally negative eigenvalues of $-N$ are mapped to eigenvalues of D_{zw} that are strictly smaller in magnitude than one. Based on (10) we propose direct parameterization satisfying $N \succ 0$, enabling unconstrained optimization.

To guarantee Condition 5 through D_{zw} defined according to (10) with $N \succ 0$, we use the parameterization

$$N = \Psi(D_A^\top D_A + D_B - D_B^\top + \epsilon I), \quad (11)$$

where the matrix $\Psi = \text{diag}(e^{D_d})$ such that N is constructed with the free variables $D_A \in \mathbb{R}^{n_w \times n_w}, D_B \in \mathbb{R}^{n_w \times n_w}$ and $D_d \in \mathbb{R}^{n_w}$ and a constant $0 < \epsilon \ll 1$. By combining a symmetric positive-semi-definite term $D_A^\top D_A$, a skew-symmetric term $D_B - D_B^\top$ and a strictly positive definite term ϵI , with positive scaling by Ψ , N is guaranteed to be strictly positive-definite by construction. The positive scaling term Ψ is shown in Revay et al. (2020) to extend the feasible domain of N . Additionally, it aids in counteracting potential poor scaling of variables which can be introduced through the transformation (10).

When considering the use of LPV-LFR models in identification, the parameterization of N according to (11) enables unconstrained optimization without risk of obtaining ill-posed models. By substituting the direct free parameterization of D_{zw} with the transformed free variables in D_A, D_B and D_d for constructing D_{zw} , the number of parameters is increased from n_w^2 to $2n_w^2 + n_w$. However, as noted in Winston and Kolter (2020), by populating only the lower triangular elements of D_A and the strictly upper triangular elements of D_B , this overparameterization is greatly reduced, now requiring only $n_w^2 + n_w$ elements, n_w variables more than populating D_{zw} directly.

4. IDENTIFICATION METHOD

4.1 Parameter Estimation

We aim to estimate a parametric surrogate model using LFR parameterization (6), given a dataset \mathcal{D}_N by minimizing the criterion:

$$V_N^{\text{fit}}(\theta, \mathcal{D}_N) = \frac{1}{N} \sum_{k=0}^{N-1} \|\hat{e}_{k|\theta}\|_2^2, \quad (12)$$

where $\hat{e}_{k|\theta} = y_k - \hat{y}_{k|\theta}$ represents the prediction error given the parameters θ . By choosing the model structure in (6), with *Output-Error* (OE) noise model, the prediction error equals the simulation error.

The parameter vector θ is comprised of the combined parameter vectors of the plant and scheduling map, $\theta = [\theta_G^\top \theta_\psi^\top]^\top$. The minimization of (12) matches the classical PEM criterion which aims to minimize the *Mean Squared Error* (MSE) of the predictions. This leads to the following optimization problem:

$$\begin{aligned} \underset{\theta}{\text{argmin}} \quad & V_N^{\text{fit}}(\theta, \mathcal{D}_N) + \rho \|\theta\|_2^2, \\ \text{s.t.} \quad & x_0 = \theta_{x_0}, \\ & \hat{p}_k = \hat{\psi}(\hat{x}_k, u_k, d_k, \theta), \\ & \hat{x}_{k+1} = \mathcal{A}(\Delta(\hat{p}_k), \theta) \hat{x}_k + \mathcal{B}(\Delta(\hat{p}_k), \theta) u_k, \\ & \hat{y}_k = \mathcal{C}(\Delta(\hat{p}_k), \theta) \hat{x}_k + \mathcal{D}(\Delta(\hat{p}_k), \theta) u_k, \\ & \hat{e}_k = y_k - \hat{y}_k, \end{aligned} \quad (13)$$

where θ_{x_0} represents the initial state as additional decision variable and where $\rho \|\theta\|_2^2$ is added as an ℓ_2 -regularization term. To solve this optimization problem, we leverage the approach described in Bemporad (2025) based on JAX (Bradbury et al. (2018)). In this gradient-based method, local optimization is performed in two steps. First, a fixed number of iterations is taken using the Adam algorithm, followed by a number of iterations using the *bound-constrained limited-memory Broyden-Fletcher-Goldfarb-Shanno* (L-BFGS-B) algorithm (Liu and Nocedal (1989)). The use of Adam, through the incorporation of *momentum*, aids in escaping local minima at the early iterations of the optimization process, providing a better point of initialization for the L-BFGS-B optimizer, which subsequently converges accurately to the final minimum of the optimization process. This two-step approach has been shown to be computationally efficient for the identification of NL-SS systems (Bemporad (2025)) as well as self-scheduled LPV-SS models (Bemporad and Tóth (2025)), particularly when compared with methods using Adam exclusively.

4.2 Parameter Initialization

When starting the optimization procedure, initial values for all elements in the parameter vector are required. This is done in a pseudo-random manner. The elements of the plant are initialized as follows:

$$\begin{aligned} A_x &= 0.5I, & B_w &= \mathbf{0}, \\ B_u &\sim \mathcal{U}(-0.1, 0.1), & C_z &\sim \mathcal{U}(-0.1, 0.1), \\ D_{zu} &\sim \mathcal{U}(-0.1, 0.1), & C_y &\sim \mathcal{U}(-0.1, 0.1), \\ D_{yw} &= \mathbf{0}, & D_{yu} &= \mathbf{0}. \end{aligned} \quad (14)$$

If affine LPV-LFR models are used, D_{zw} is left out of the parameter vector, fixed at a zero matrix. For well-posed rational LPV-LFR models, we construct the D_{zw} matrix by drawing lower triangular elements from a uniform distribution $\mathcal{U}(0, 0.1)$ for the matrix D_A , the strictly upper triangular elements of D_B follow the normal distribution $\mathcal{N}(1, 1)$, finally $D_d = \mathbf{0}$ is chosen to initialize the remainder of the parameter vector. Lastly, to initialize the parameters of the scheduling map, represented by a ResNet, uniform

Xavier initialization (Glorot and Bengio (2010)) is used. Bias terms are initialized as zero.

5. SIMULATION EXAMPLES

To evaluate the performance of the identified models, we consider two simulation examples. First, a *Nonlinear Mass-Spring-Damper* (NL-MSD) system is considered to evaluate the trade-off of rational-scheduling dependency. Secondly, we consider a *Control Moment Gyroscope* (CMG), previously used to evaluate performance of joint-estimation methods, enabling comparison of the proposed methodology to existing methods. As a performance measure, the *Best Fit Rate* (BFR) is considered, defined as:

$$\text{BFR} = \max \left\{ 1 - \frac{\sum_{k=0}^{N-1} \|y_k - \hat{y}_k\|_2}{\sum_{k=0}^{N-1} \|y_k - \bar{y}\|_2}, 0 \right\} \cdot 100\%, \quad (15)$$

where \hat{y}_k is the estimated output and \bar{y} is the sample mean of y .

The LPV-LFR models of both examples are trained according to the same optimization strategy proposed in Section 4. Leveraging the efficiency of the JAX-based method, all models are trained for 100 random initializations on an Intel 14700K CPU, and the model with the highest BFR on validation data is selected.

5.1 Nonlinear Mass-Spring-Damper

To illustrate the trade-off between affine and rational-dependency LPV-LFR models we show a numerical example based on a DT NL-MSD system described by:

$$\begin{aligned} x_{1,k+1} &= x_{1,k} + T_s x_{2,k}, \\ x_{2,k+1} &= x_{2,k} + \frac{T_s}{m} \left(u_k - \frac{3}{5} x_{1,k} u_k - k_1 x_{1,k} - k_2 x_{1,k}^3 - d_1 x_{2,k} \right), \\ y_k &= x_{1,k}, \end{aligned} \quad (16)$$

with $T_s = 0.1$, $m = 1$, $k_1 = 0.1$, $k_2 = 1$, $d_1 = 1$ and where x_1 represents the position of the system and x_2 its velocity. This plant features nonlinearities dependent on x_1 and x_1^2 , requiring two scheduling variables for affine LPV representations or one scheduling variable for rational dependency models.

The Data: Using the DT system, we generate three datasets, one training, validation and test set. Each dataset is generated by exciting the system (16) with a different realization of a random phase multisine signal. The training and validation input signals are $N = 6 \cdot 10^3$ samples long, the test set is longer, consisting of $N = 3 \cdot 10^4$ samples. Each input has frequency components from $\frac{1}{6}$ Hz to 5 Hz. The input signals have amplitudes with standard deviation $\sigma_u = 4$ N. The output of (16) has additive white noise $\mathcal{N}(0, \sigma_e^2)$ with $\sigma_e^2 = 0.063$, resulting in a SNR of approximately 20 dB.

Model Settings: To compare the performance of rational and affine-dependency based LPV-LFR models, we train such models using the well-posed parameterization with $(n_x = 2, n_p = 1, \eta = 3)$, matching the required order necessary for rational models. Subsequently we train affine models with $(n_x = 2, n_p = 2, \eta = 1)$ matching the theoretically required dimensions for affine models. On this example, linear scheduling maps with saturation:

$$\hat{\psi}(x, u) = \tanh(W_x x + W_u u + b), \quad (17)$$

Table 1. Results on the NL-MSD example using LPV-LFR models.

Model	BFR train	BFR val	BFR test	time
True System	89.47	90.19	90.15	-
Affine ($n_p=1$)	53.56	41.78	44.90	37 s
Affine ($n_p=2$)	89.56	90.20	89.87	87 s
Rational ($n_p=1$)	89.57	90.20	90.16	112 s

are considered. Here W_x, W_u, b are free variables. Each model is trained for 1000 Adam epochs followed by 4000 epochs using L-BFGS.

Results: The results achieved on the NL-MSD benchmark are shown in Table 1 and illustrated in Figure 1. They show that LPV-LFR models with affine and rational scheduling dependency are capable of achieving accurate results on test data-set. However, given the simple scheduling map (17), the affine models require a higher scheduling dimension $n_p = 2$ to achieve the same accuracy as the LPV-LFR model with rational scheduling dependency achieves with a scheduling dimension of one. This illustrates the trade-off between complexity in terms of scheduling dimension and complexity in terms of scheduling dependency which is made possible through the well-posed parameterization introduced in this work.

5.2 Control Moment Gyroscope

As second simulation example, we consider the 3-DOF CMG and compare achieved performance with the methods presented in Verhoek et al. (2022) and Bemporad and Tóth (2025). The 3-DOF CMG, as shown in Figure 2, consists of a disk mounted inside a blue gimbal, which in turn is mounted inside a red gimbal which is mounted inside of silver gimbal. The disk, and gimbals are each equipped with a DC motor for actuation and an encoder to measure the angular positions (q_1, q_2, q_3 and q_4 for the disk, blue, red, and silver gimbal respectively). During the simulation, the red gimbal is locked at $q_3 = 0$, the blue gimbal q_2 is actuated with a motor current i_2 , and the angular velocity of the silver gimbal \dot{q}_4 is measured and considered as output. The velocity of the disk \dot{q}_1 is controlled independently, tracking a random multi-level-reference signal with amplitudes between 30 and 50 rad/s and dwell time of 4-8 seconds. The resulting dynamics can, for small angles of q_2 , be interpreted as a nonlinear SISO model between the input i_2 and output \dot{q}_4 with dynamics dependent on the external input \dot{q}_1 .

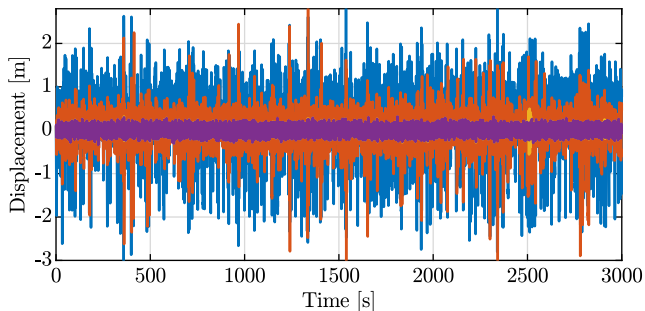


Fig. 1. True output (—), affine LPV-LFR ($n_p=1$) sim. error (—), affine LPV-LFR ($n_p=2$) sim. error (—), and rational LPV-LFR sim. error (—) on the test data of the NL-MSD.

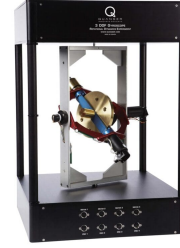


Fig. 2. Picture of the CMG considered in example 2.

The Data: As Verhoek et al. (2022) describes, the input of the first gimbal is excited with a sinusoidal carrier wave with white noise added: $u_k = \frac{1}{2} \sin(\omega T_s k) + v_k$ where $v_k \sim \mathcal{N}(0, \sigma_v^2)$ and $\sigma_v = \frac{1}{3}$. For each dataset, the frequency of the sinusoidal carrier wave is drawn from a uniform distribution, $\omega \sim \mathcal{U}(1, 2)$. Furthermore, an OE noise structure is considered with error signal $e_k \sim \mathcal{N}(0, \sigma_e^2)$ with variance $\sigma_e^2 = 2.2 \cdot 10^{-5}$ corresponding to a SNR of 35 dB. The velocity of the disk follows the previously specified reference. The data is generated using CT simulation with RK4 integration and is subsequently down-sampled to 100 Hz. A training set consisting of 10^4 samples is created as well as a validation set of $3 \cdot 10^4$ samples.

Model Settings: To compare the performance of the proposed LPV-LFR-based approach with the methods described in Verhoek et al. (2022) and Bemporad and Tóth (2025), we opt to train models with the same state and scheduling dimension ($n_x = 5, n_p = 3$). Rational-dependency and affine-dependency-based models are trained for comparison, both with $\eta = 1$. As scheduling map, 2-hidden layer ResNets with 6 neurons per hidden layer and tanh activation functions are used. Each model is trained for 2000 epochs using Adam, followed by 4000 epochs using L-BFGS.

Results: The simulation performance of the LTI, affine LPV-LFR and rational LPV-LFR model are shown in Figure 3 and compared with the results in Bemporad and Tóth (2025) in Table 2. The results show that for affine models, results similar to existing joint-estimation methods can be achieved, for rational models however, performance is slightly worse. This reduction in performance is attributed to the increased complexity of the optimization problem, resulting from the additional complexity of the rational scheduling dependency.

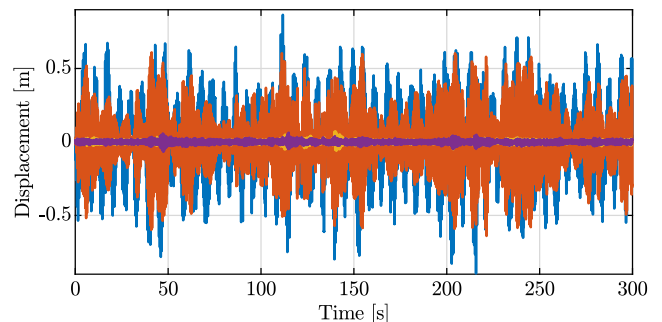


Fig. 3. True output (—), LTI sim. error (—), affine LPV-LFR sim. error (—), and rational LPV-LFR sim. error (—) on the validation data of the CMG.

Table 2. Comparison of LPV identification results on the CMG dataset. Previous results are taken from Bemporad and Tóth (2025) and achieved on different hardware, computation times may differ. The LPV-SUBNET method is described in Verhoek et al. (2022).

Model	BFR train	BFR val	time
True System	98.16	98.19	-
Affine LPV-LFR	97.46	96.41	172 s
Rat. LPV-LFR	97.12	96.02	279 s
LPV-SS	97.61	96.50	47.54 s
LPV-SUBNET	97.28	96.40	≈ 10 h

6. CONCLUSION

This work has proposed the use of the linear fractional representation for LPV models in the joint-estimation of LPV models and scheduling maps. A novel parameterization which, by construction, guarantees well-posedness of LPV-LFR models with rational scheduling dependency, has been introduced. The well-posed parameterization has been shown to be capable of accurately modelling nonlinear systems a simulation example, illustrating how the rational scheduling dependency can reduce the required scheduling order. Finally, estimation of LPV-LFR models with affine and rational-dependency has been compared to state-of-the-art joint-estimation methods for LPV models on a benchmark where LPV-LFR models have been shown to achieve results close to existing methods.

REFERENCES

- Bemporad, A. (2025). An L-BFGS-B approach for linear and nonlinear system identification under ℓ_1 and group-lasso regularization. *IEEE Transactions on Automatic Control*.
- Bemporad, A. and Tóth, R. (2025). Efficient identification of linear, parameter-varying, and nonlinear systems with noise models. *arXiv preprint arXiv:2504.11982*.
- Bianchi, F.D. and Sánchez-Peña, R.S. (2010). Robust identification/invalidation in an LPV framework. *International Journal of Robust and Nonlinear Control*, 20(3), 301–312.
- Bradbury, J., Frostig, R., Hawkins, P., Johnson, M.J., Leary, C., Maclaurin, D., Necula, G., Paszke, A., VanderPlas, J., Wanderman-Milne, S., and Zhang, Q. (2018). JAX: composable transformations of python+numpy programs. <https://github.com/google/jax>.
- Cheng, Y. and Sznaier, M. (2015). Identification of LPV systems with LFT parametric dependence via convex optimization. In *Proc. of the 54th IEEE Conference on Decision and Control*, 1459–1464. Osaka, Japan.
- Cox, P.B. and Tóth, R. (2021). Linear parameter-varying subspace identification: A unified framework. *Automatica*, 123, 109296.
- den Boef, P., Cox, P.B., and Tóth, R. (2021). LPVcore: MATLAB toolbox for LPV modelling, identification and control. In *Proc. of the 19th IFAC Symposium on System Identification*, 385–390.
- Glorot, X. and Bengio, Y. (2010). Understanding the difficulty of training deep feedforward neural networks. In *Proc. of the 13th International Conference on Artificial Intelligence and Statistics*, 249–256. JMLR Workshop and Conference Proceedings, Sardinia, Italy.
- He, K., Zhang, X., Ren, S., and Sun, J. (2016). Deep Residual Learning for Image Recognition. In *Proc. of the IEEE Conference on Computer Vision and Pattern Recognition*, 770–778. Las Vegas, USA.
- Hjartarson, A., Seiler, P., and Packard, A. (2015). LPV-Tools: A Toolbox for Modeling, Analysis, and Synthesis of Parameter Varying Control Systems. In *Proc. of the 1st IFAC Workshop on Linear Parameter Varying Systems*, 139–145. Grenoble, France.
- Hoffmann, C. and Werner, H. (2014). Complexity of Implementation and Synthesis in Linear Parameter-Varying Control. In *Proc. 19th IFAC World Congr.* Cape Town, South Africa.
- Lee, L.H. and Poolla, K. (1999). Identification of Linear Parameter-Varying Systems Using Nonlinear Programming. *Journal of Dynamic Systems, Measurement, and Control*, 121(1), 71–78.
- Liu, D.C. and Nocedal, J. (1989). On the limited memory BFGS method for large scale optimization. *Mathematical Programming*, 45(1-3), 503–528.
- Mejari, M., Piga, D., Toth, R., and Bemporad, A. (2019). Kernelized Identification of Linear Parameter-Varying Models with Linear Fractional Representation. In *Proc. of the 18th European Control Conference*, 337–342. Naples, Italy.
- Mohammadpour, J. and Scherer, C.W. (eds.) (2012). *Control of Linear Parameter Varying Systems with Applications*. Springer US, Boston, MA.
- Nemani, M., Ravikanth, R., and Bamieh, B. (1995). Identification of linear parametrically varying systems. In *Proc. of the 34th IEEE Conference on Decision and Control*, 2990–2995. New Orleans, LA, USA.
- Revay, M., Wang, R., and Manchester, I.R. (2020). Lipschitz Bounded Equilibrium Networks. *arXiv preprint arXiv:2010.01732*.
- Scherer, C.W. (2001). LPV control and full block multipliers. *Automatica*, 37, 361–375.
- Scherer, C. and Weiland, S. (2015). Linear matrix inequalities in control. *Lecture Notes*.
- Tóth, R. (2010). *Modeling and Identification of Linear Parameter-Varying Systems*, volume 403 of *Lecture Notes in Control and Information Sciences*. Springer, Berlin, Heidelberg.
- Van Wingerden, J.W. and Verhaegen, M. (2009). Subspace identification of Bilinear and LPV systems for open- and closed-loop data. *Automatica*, 45(2), 372–381.
- Verhoek, C., Beintema, G.I., Haesaert, S., Schoukens, M., and Toth, R. (2022). Deep-Learning-Based Identification of LPV Models for Nonlinear Systems. In *Proc. of the 61st IEEE Conference on Decision and Control*, 3274–3280. Cancun, Mexico.
- Verhoek, C., Wang, R., and Tóth, R. (2023). Learning Stable and Robust Linear Parameter-Varying State-Space Models. In *Proc. of the 62nd IEEE Conference on Decision and Control*, 1348–1353. Singapore.
- Winston, E. and Kolter, J.Z. (2020). Monotone operator equilibrium networks. *Advances in neural information processing systems*, 33, 10718–10728.
- Zhou, K., Doyle, J., and Glover, K. (1996). Robust and optimal control. *Control Engineering Practice*, 4(8), 1189–1190.